Effect of Limestone Fillers on Ca-Leaching and Carbonation of Cement Pastes

Article *in* Key Engineering Materials · September 2016

DOI: 10.4028/www.scientific.net/KEM.711.269

5 authors, including:

Quoc Tri Phung
Belgian Nuclear Research Centre
28 PUBLICATIONS **76** CITATIONS
SEE PROFILE

Norbert Maes
Belgian Nuclear Research Centre
117 PUBLICATIONS **698** CITATIONS
SEE PROFILE

Diederik Jacques
Belgian Nuclear Research Centre
212 PUBLICATIONS **2,046** CITATIONS
SEE PROFILE

Guang Ye
Delft University of Technology
237 PUBLICATIONS **1,980** CITATIONS
SEE PROFILE

Key Engineering Materials
ISSN: 1662-9795, Vol. 711, pp 269-276
doi:10.4028/www.scientific.net/KEM.711.269

Online: 2016-09-20

Effect of Limestone Fillers on Ca-Leaching and Carbonation of Cement Pastes

Quoc Tri PHUNG [1,a *], Norbert MAES [1,b], Diederik JACQUES [1,c], Geert DE SCHUTTER [2,d], and Guang YE [2,3,e]

[1]EHS Institute, Belgian Nuclear Research Centre (SCK•CEN), Belgium

[2]Magnel Laboratory for Concrete Research, Ghent University, Belgium

[3]Microlab, Delft University of Technology, The Netherlands

[a]qphung@sckcen.be, [b]nmaes@sckcen.be, [c]djacques@sckcen.be, [d]geert.deschutter@ugent.be, [e]g.ye@tudelft.nl

Keywords: carbonation; leaching; microstructure; limestone fillers; cement paste

Abstract: Because of its environmental and economic benefits, part of cement is replaced by limestone fillers (LS). However, the effect of LS on the chemical degradation of cement-based materials is still unclear. In this study, accelerated leaching and carbonation were applied on cement pastes to study the effects of LS replacement on the degradation rates and microstructural alterations of degraded materials. Ammonium nitrate solution was used to accelerate the leaching process, while carbonation was speeded up by applying an elevated pressure gradient of pure CO_2 on samples with 65% relative humidity. The carbonation rate was characterized by phenolphthalein carbonation depth and CO_2 uptake, while leaching rate was quantified by phenolphthalein leaching depth and Ca-leached amount. Leached/carbonated samples were analyzed by a series of post-analysis techniques to characterize the microstructural and mineralogical changes. Results showed that, for a similar w/c ratio, a higher LS replacement resulted in lower leaching rate. For carbonation, LS replacement promoted the CO_2 uptake despite similar carbonation depth. Furthermore, LS replacement led to less C-S-H carbonation compared to samples without LS.

Introduction

Many environments to which concrete is exposed are highly aggressive due to various chemical components. In such environments, concrete is subjected to processes of chemical degradation (e.g. carbonation, leaching). Chemical degradation is typically the result of alteration of the cement matrix mineralogy caused by interacting with an aggressive environment. The interaction disturbs the equilibrium between the pore solution and the solid phases of the cement matrix which results in dissolution and/or precipitation of minerals. The chemical degradation of cementitious materials is mostly followed by a weakening of the material and the alteration of the microstructure.

The carbonation process in cement-based materials results in a pH decrease. The development of lower alkaline environment accelerates the corrosion of reinforcing bars in concrete because of dissolution of the thin oxide passive layer protecting the steel bars from corrosion. Ca-leaching is one of the most serious degradation processes in concrete and reinforced concrete structures for the very long-term (nuclear waste disposal system) or in hydro structures but despite the long history of concrete, it has only been studied since the 1980s. Leaching of cement-based materials changes its properties such as a reduction in pH, an increase in porosity and transport properties and detrimental effects on properties related to long-term durability.

Beside extrinsic factors, there are many intrinsic factors influencing carbonation and leaching including: water/cement (w/c) ratio, cement type, supplementary cementing materials and LS replacement. Few researchers [1-3] have studied these factors, but many questions still remain, especially about the effects of LS replacement on carbonation and leaching, thought replacing part of cement by limestone fillers is getting more attention in recent years because of its environmental and economic benefits. Some authors state that concrete with LS replacement increases the

carbonation rate compared to concrete with the same water/powder (w/p) ratio [4, 5]. On the contrary, Tsivilis et al. [6] showed that the carbonation resistance does not decrease even with 35% LS replacement, while Lollini et al. [7] showed a remarkable drop of the carbonation resistance for 30% replacement and no clear effect at 15% replacement. LS is also expected to have an effect on Ca-leaching of cementitious materials. However, information is still missing in the literature.
In the present study, the newly developed carbonation method and accelerated leaching in ammonium nitrate [8] was applied to investigate the effects of LS replacement on microstructural and mineralogical alterations after degradation. An integrated analysis of samples with and without LS at different w/p ratios before and after degradation was performed in order to identify how processes at the micro scale are influenced by LS replacement.

Experimental descriptions

Materials. All experiments were performed on cement pastes made from cement, tap water and LS. Type I OPC cement (CEM I 52.5 N) was used. Limestone filler used had a $CaCO_3$ content of 98.30%. Superplasticizer Glenium 27 was added to the mix with content of 0.5% w.r.t. mass of cement.
In order to investigate the effects of LS, three sets of cement pastes were cast in a temperature-controlled room of 21 ± 1°C: sample C0 with w/p ratio of 0.425, 0% of LS replacement; C10 with w/p ratio of 0.375 and 10% of LS replacement, and C20 with w/p ratio of 0.325 and 20% of LS replacement. Note that all samples had quite similar w/c ratios of 0.415 ± 0.01. The carbonated and leached samples are named C0-C, C10-C, C20-C and C0-L, C10-L, C20-L, respectively.
Cement pastes were poured in a PVC tube with an inner diameter of 97.5 mm [9]. After 28 days of curing in sealed condition, it was sawn into small slices of 25 mm thick. Prior to the carbonation experiment, the cement slices were conditioned to a target internal relative humidity (RH) of 65% to have optimal conditions for fast carbonation. For leaching experiment, the cement slices were saturated in a saturated lime solution to avoid initial leaching following the procedure described in [10]. The slices were only allowed for 1D leaching at the bottom and top of the slices.
Accelerated carbonation. A new method [11] in which an elevated pressure gradient of pure CO_2 was applied to samples at a controlled internal RH to take into account the contribution of advective flow was used to accelerate the carbonation. CO_2 pressure was increased at one sample side, while the other side was balanced to atmospheric pressure. A constant absolute pressure of 6 bar was applied in order to have at one hand a sufficient high pressure of pure CO_2 to reduce the experimental time, but on the other hand, to reduce the risk for inducing micro cracks in the cement paste by applying a too high pressure. The amount of carbon dioxide reacting with the cement was derived from measurements with two mass flow meters (see Fig. 1a). A carbonation test was performed for a period of 4 weeks.

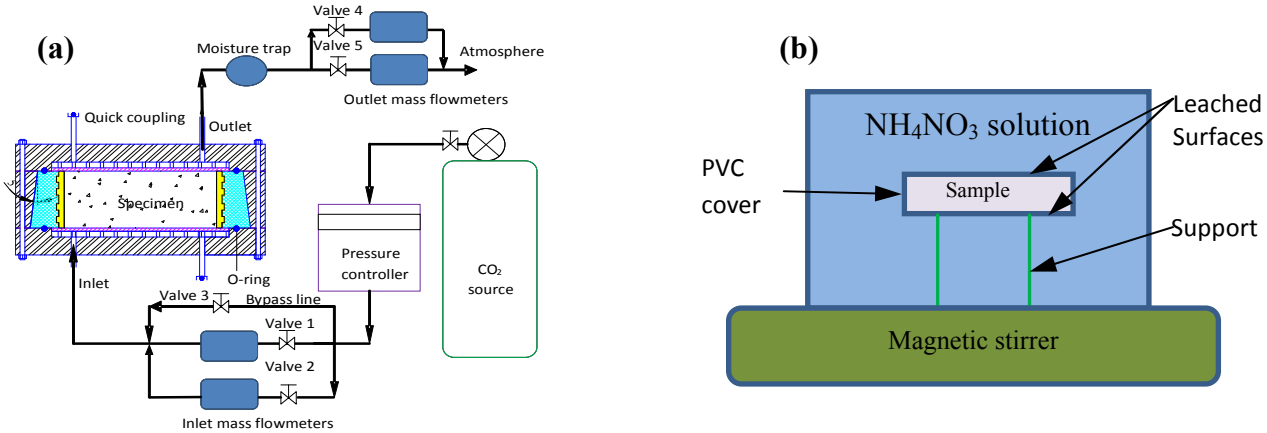

Fig. 1. Test setups for accelerated carbonation using pressure gradient of pure CO_2 (a) [11] and accelerated leaching using NH_4NO_3 solution (b) [9]

Accelerated Ca-leaching. The saturated cement slices were immersed in 6M NH_4NO_3 solution chambers [12] (see Fig. 1b). The ratio between NH_4NO_3 solution over the contact surface area of the sample was 8 cm^3/cm^2. Such a factor was chosen to maintain leaching acceleration without renewal of solution because the solution is used for quantitative analysis of the Ca-leached amounts. Nitrogen was bubbled through the system to prevent carbonation during leaching and to remove the formed NH_3 gas. The solution was homogenized by a magnetic stirrer.

Characterization of degraded materials. The leaching tests were stopped at different testing time (7, 14, 21, and 28 days) to examine different leaching grades. The broken leached samples were sprayed by a phenolphthalein solution to determine the leached depth. For carbonation, the carbonated depth was only measured at the end of experiments (28 days). The amount of leached calcium was measured by ion chromatography in solutions extracted on a weekly basis from the setup. Different post-analysis techniques were used to characterize the microstructural and mineralogical changes. The combination of mercury intrusion porosimetry (MIP) and N_2-adsorption [12] was used to measure porosity, pore size distribution and specific surface area. This method enables to characterize pore structural changes over a broad pore size range where MIP gives reasonable results for larger pore sizes, while N_2-adsorption provides information on the smaller pores. X-ray diffraction (XRD) was used to identify the phase changes. Quantitative XRD was performed on powder samples with 10% of ZnO internal standard material addition in order to identify the change of portlandite (CH) content after leaching. Thermal gravimetric analysis (TGA) was applied for carbonated samples. Note that for leached materials, TGA could not be applied because the decomposition of $Ca(NO_3)_2$ coincides with decomposition of other phases. Details of characterisation techniques can be found in [12].

Results

Degraded depth. The leached depth linearly increased with the square root of immersion time in NH_4NO_3 as shown in Fig. 2a. This is one of the indicators which illustrates that leaching in ammonium nitrate solution is a diffusion controlled phenomenon. At similar w/c ratio, the propagation rate of leached depth is clearly decreased with the increase of limestone filler replacement.

The carbonation depths determined by phenolphthalein spraying are also presented in Fig. 2a. However, the depths were only measured after 28-day carbonation. The carbonation depths obtained were quite similar for all samples: C0-C (2.7 mm), C10-C (2.5 mm) and C20-C (2.3 mm). The effect of limestone filler on carbonation depth is not clear through the trend (decrease in degraded depth with the increase of limestone filler) as leached depth is still preserved.

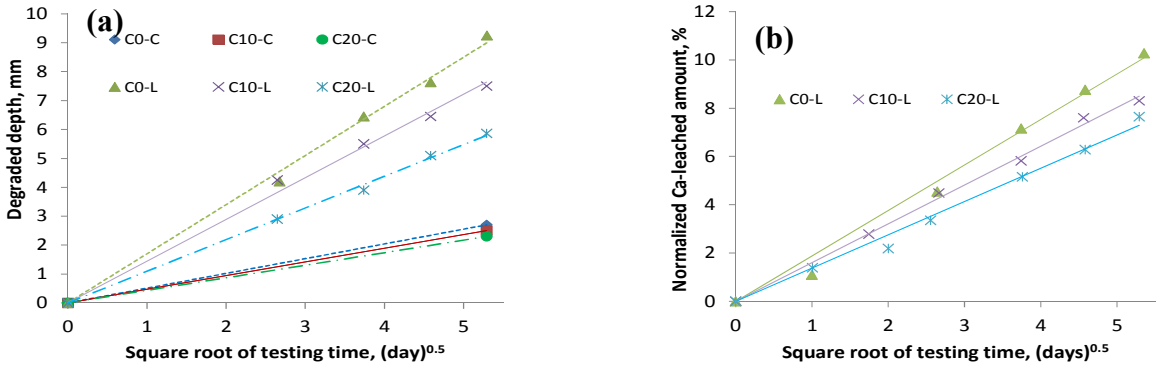

Fig. 2. Increase of carbonated/leached depth (a) and normalized Ca-leached amount to cement (b) over time

Ca-leached amount and CO_2 uptake . Fig. 2b presents the amount of leached calcium normalized to the cement content of the samples before leaching. Again, a linear relation of Ca-leached amount over square root of time was observed similar to the propagation of the leached depth. Increasing limestone filler also results in a decrease in the Ca-leached amount.

The CO_2 uptake is defined as the mass ratio between the CO_2 which reacted with the sample and the cement in the sample, expressed as:

$$Uptake_{CO_2} = \frac{\left(m_{CO_2}^{inlet} - m_{CO_2}^{outlet}\right)}{cem} 100\% \quad (1)$$

where $m_{CO_2}^{inlet}$ and $m_{CO_2}^{outlet}$ [kg] are the mass of CO_2 measured by inlet and outlet mass flow meters, respectively; *cem* is the cement mass in the sample [kg].

Fig. 3 shows the CO_2 uptake of sample C0-C, C10-C, and C20-C during 28 days of carbonation. The CO_2 uptake rate was initially very fast but decreased significantly after a few hours of carbonation. Initially, CO_2 mainly penetrated into the sample via the gaseous phase. As carbonation proceeds, the released water increased the saturation degree of the sample. At a certain time, the sample was getting saturated close to the inlet which prevented further gaseous transport. The porosity reduction (showed later) also contributes to a slower CO_2 transport. From the moment of saturation of the first thin layer, the carbonation rate dramatically dropped. The longer the experimental time, the lower the carbonation rate because the released water tends to saturate the entire sample, hence slowing down the (gaseous) CO_2 transport.

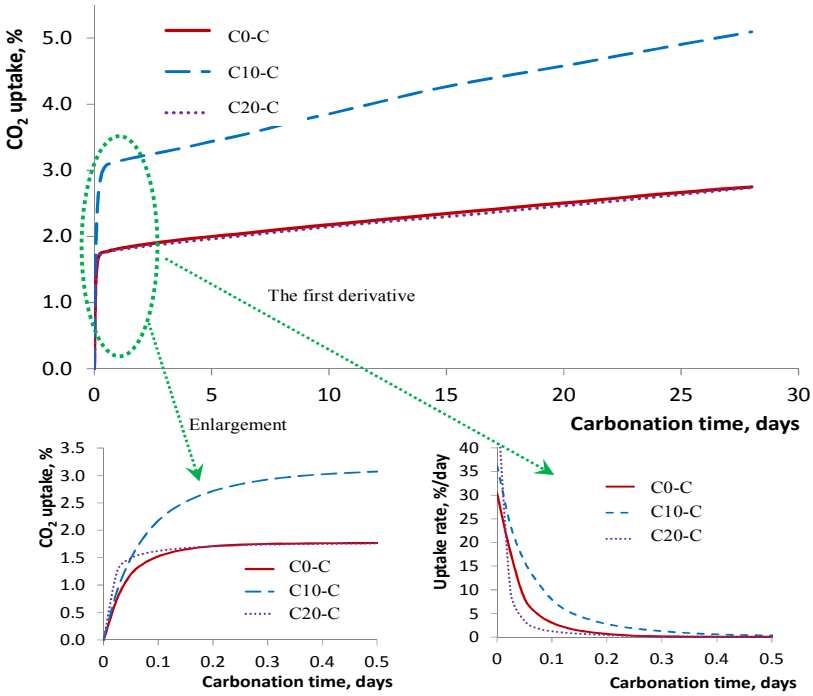

Fig. 3. CO_2 uptake (in percentage wrt. cement mass in sample) as a function of carbonation time – the first derivative curves (bottom) show a decrease in carbonation rate over time.

The total CO_2 uptakes of C0-C and C20-C were similar despite its different initial uptake rates. Sample C0 had a higher w/p ratio but quite similar water permeability (results shown in [9]) compared to sample C20, which could result in the same residual CO_2 uptake. Both initial and residual CO_2 uptake rates were the highest for C10-C, but major difference was found in the initial carbonation stage. This indicates that the CO_2 advection in the gaseous phase during the initial carbonation and diffusion in the aqueous phase after the initial carbonation were the fastest in C10-C. For sample with LS (C10-C), calcite may precipitate preferentially on limestone particles than on portlandite and C-S-H phases as explained in [11], which promotes the CO_2 uptake. Additionally, the dilution effect does contribute to larger CO_2 uptake of C10-C compared C0-C (i.e. more cement in C0). However if the LS replacement is increased from 10% (sample C10) to 20% (sample C20), the limestone filler no longer promotes the CO_2 uptake. The CO_2 uptake of C20-C was significantly smaller than C10-C as a result of higher LS replacement (lower w/p).

Mineralogical changes. Fig. 4 (top) presents the XRD patterns for carbonated and reference samples for the first 3 mm from the inlet. Presence of portlandite is indicated by the peaks at 2θ =

17.9° and 34.2°. There is an intense peak at 29.4° corresponding to calcite which was formed during carbonation. Note that the intense peak of calcite in reference samples C10 and C20 is due to the LS replacement. Interesting is the peak of vaterite in carbonated samples C0-C and C10-C even with relatively low intensity. The formation of vaterite is favoured when the system has a low Ca^{2+}/CO_3^{2-} concentration ratio [13, 14] which is the case of accelerated carbonation. Furthermore, the carbonation of ettringite leads to the formation of vaterite crystals [15]. The XRD patterns indicate ettringite dissolution as ettringite peaks are more visible in the reference samples than in the carbonated samples in most cases. Fig. 4 (bottom) shows the XRD patterns for leached and reference samples. It is clearly observable that CH was completely dissolved in all leached samples. There are two intense peaks of CH for the reference samples which totally disappear after leaching. Except for C-S-H, which cannot be detected, the most visible phases in the XRD patterns of the leached samples are calcite, ettringite and unhydrated cement which indicate that they are hardly degraded by the NH_4NO_3 solution. No new crystalline phases were observed as for leaching in deionized water. This underpins the statement that leaching in NH_4NO_3 results in same end-products, as obtained for "natural" leaching. Percentage of CH and calcite in the reference and carbonated samples was determined by TGA using the tangent method in order to take into account the gradual decomposition of C-S-H. Fig. 5 shows that in C0-C and C10-C, CH and calcite, respectively, gradually decreases and increases. CH was observed in the first sampling interval (0-3 mm) although the phenolphthalein test indicated a pH lower than 9 in that interval (2.7 and 2.5 mm for C0-C and C10-C, respectively). It is hypothesized here that under accelerated conditions in which the transport of CO_2 is faster than Ca ions, a calcite layer may form around the CH (or C-S-H) particles. Two main consequences are that (i) these CH particles are not easily accessible for CO_2 and thus further carbonation is extremely limited, and (ii) the pH of the pore solution is no longer buffered by CH. The calcite formed from C-S-H carbonation was estimated as the difference between the calcite content measured by TGA and the calcite formed from CH. The estimation showed that C-S-H carbonation contributes 41.8%, 33.3% and 4.6% to calcite formation in the intervals 0-3, 3-6 and 6-9 mm for S3C, respectively. The carbonation of C-S-H in C10-C was limited to 15.5% and 6.4% in the intervals 0-3 and 3-6 mm, respectively (Fig. 6). There was no C-S-H carbonation observation beyond those depths. The quantitative XRD results of 28-day leached samples C0-L and C10-L are also shown in Fig. 5. There was no portlandite detected within 6 mm depth from the exposed surface which is consistent with the degraded depth determined by phenolphthalein spraying. However, beyond the leached depth (9.25 mm and 7.5 mm for C0-L, and C10-L, respectively), the amount of portlandite was smaller than the one in reference. In the interval 9-12 mm, the portlandite content was still slightly reduced compared to reference samples. This indicates that leaching does not result in a sharp degradation front. Portlandite still dissolves beyond the phenolphthalein degraded depth.

Microstructural changes. Fig. 7 compares the porosity of leached, carbonated and reference samples determined by the combined MIP and N_2-adsorption method. In the range of 3 nm - 100 μm, the porosity of leached samples hugely increased, from 68% up to 159% compared to the porosity of reference samples. The higher LS replacement, the larger porosity increases. Such a large porosity increase is not only due to the decalcification of CH but also due to (partial) decalcification of the C-S-H system. In all leached samples, the cumulative pore volume curves exhibited two ranges of significant porosity increase. The first range was situated in the 60 nm – 500 nm pore sizes corresponding to CH dissolution. The second ranges was smaller than 10 nm corresponding to C-S-H (and other phases) dissolution. In contrast, reference samples exhibited only one significant pore volume increase stage. The critical and threshold pore diameters were significantly shifted to bigger pore size range. Carbonation slightly reduced accessible porosity. The porosity of carbonated samples decreased about 1.3 - 2.6%. The threshold pore diameter tended to reduce. The critical pore size generally varied in a small range: C0-C and C10-C slightly decreased, while C20-C slightly increased. The specific surface areas (SSA) determined by the BET method of the leached samples significantly increased (Table 1). The specific surface area of samples with high

w/p ratios (C0-L and C10-L) increased 4-5 times after 28-day leaching in ammonium nitrate solution.

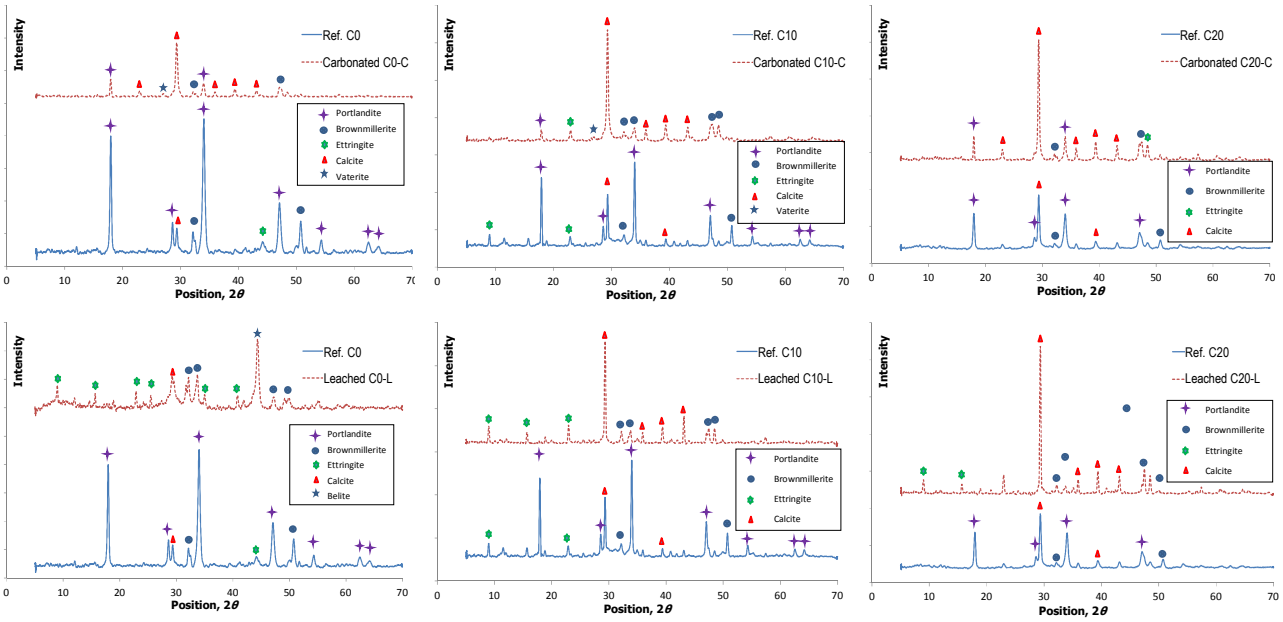

Fig. 4. XRD patterns of reference and –carbonated (top) and leached (bottom) samples taken in the first 3 mm depth from the exposed surface

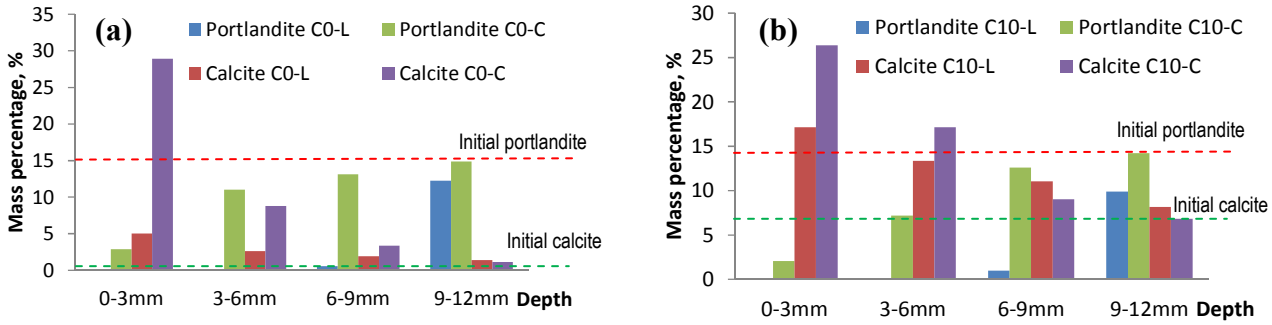

Fig. 5. Changes in portlandite and calcite contents over the depth of leached and carbonated samples C0 (a) and C10 (b) after 28 days of degradation

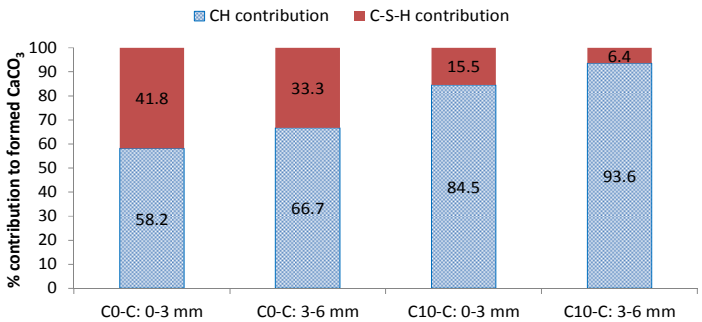

Fig. 6. Evidences of C-S-H carbonation at the depth which is near exposed surface - the carbonation of the minor phases (e.g. AFm, AFt) was negligible.

For sample with lower w/p ratio (C20-L), the SSA increased even more strongly, with a factor of 15. Such a large increase is not only attributed to the dissolution of CH but also to the dissolution of C-S-H. The gel pores of C-S-H, which have higher SSA compared to micro/mesopores made by the aggregation of the other cement components, are more easily accessible by nitrogen after leaching.

The change in SSA of carbonated samples deserves some attention. Most published studies report a decrease in SSA after carbonation. However, it is quite surprising that the BET SSA for samples without LS addition (C0-C) reasonably increased after carbonation. This observation can be explained by the opening of C-S-H gel pores or small necks of ink-bottles pores (narrow entrances

but wide bodies) as a consequence of C-S-H carbonation [11]. As indicated by the TGA results, C-S-H carbonation contributed up to 41.8% of calcite formation for sample C0-C, which was 2.5 times larger than that of sample C10-C. Both micropore volume and SSA of C0-C were increased as seen in Table 1. This means that the opening of gel pores dominates the changes of micropore structure compared to the pore filling by calcium carbonate precipitation. As the C-S-H carbonation results in lower Ca/Si ratio, the structure of C-S-H becomes more porous and accessible by nitrogen. Consequently, the SSA is expected to increase. The SSA of C-S-H is much higher than that of bulk paste but only part of this contributes to the average SSA of intact paste due to limitation in accessibility of nitrogen to small gel pores. The carbonated sample C20-C also showed a slight increase in BET SSA which may be again attributed to C-S-H carbonation.

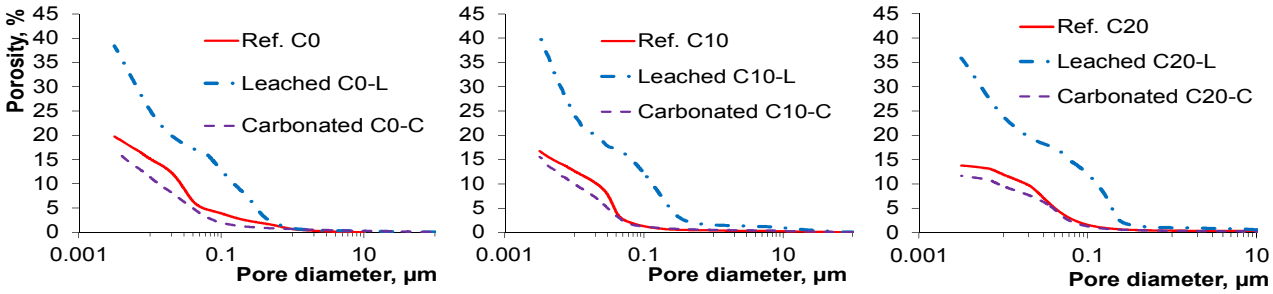

Fig. 7. Changes in porosity due to leaching and carbonation assessed by combining MIP and N_2-adsorption

The different alteration of the SSA of carbonated samples is due to differences in composition and w/p (w/c) ratio. For samples with 10 % limestone fillers C10-C, the LS can act as nucleation sites for calcite precipitation from CH carbonation. This process then limits the amount of calcite available for forming protecting layers around CH particles. Therefore, CH carbonation is favoured compared to C-S-H carbonation for samples without LS. Sample C20-C with 20% LS replacement, however, showed a slight increase of BET SSA. Probably, a small amount of C-S-H was carbonated in this case. Generally, the samples with lower w/p ratio and with LS replacement result in finer microstructures (compared to samples with the same w/c ratio). The LS may act as a nucleation site for hydration reactions given a denser pore structure with a higher hydration degree. Consequently, the accessibility of CO_2 to gel pores is limited; thereby, lower C-S-H carbonation.

Table 1. Micropore information obtained by Dubinin-Astakhov model

Sample	C0	C0-L	C0-C	C10	C10-L	C10-C	C20	C20-L	C20-C
Micropore spec. surface, m^2/g	23.7	131.6	28.8	26.4	165.4	17.5	4.2	67.9	5.0
Micropore volume, mm^3/g	11.6	65.0	14.1	12.8	82.2	8.5	2.1	32.5	2.4
Meso/micro volume ratio	6.9	3.3	4.3	3.9	2.8	5.3	12.1	4.6	8.3
BET surface area, m^2/g	30.6	145.8	38.0	34.8	182.3	23.2	6.2	86.7	7.5

Table 1 also presents the change in micropore structure of the leached materials. The micropores (smaller than 2 nm) of all leached samples were strongly affected by leaching in ammonium nitrate solution, among them the highest alteration was from the sample C20-L. Both micropore surface area and micropore volume were significantly increased during accelerated leaching. The meso/micro volume ratio was reduced after leaching which can serve as an evidence for C-S-H decalcification which resulted in higher accessibility of gel pores. For carbonation, the meso/micro volume ratio was also decreased for samples C0-C and C20-C, but less significant compared to leaching. The meso/micro volume ratio of sample C10-C increased served as an evidence for higher modification of pore structure at meso scale compared to the other samples.

Conclusions

In this study, the effects of LS replacement on the changes of microstructure and mineralogy of cement paste under accelerated carbonation and leaching were investigated. Results show that leaching and carbonation significantly change the microstructure of cementitious materials but in

different ways. The leaching significantly alters the microstructure of the cement paste to a material with a higher SSA, increased porosity and a shift to larger pore sizes. In contrast, the carbonation improves the properties of cementitious materials in terms of porosity reduction, shift of pore size distribution to smaller ranges. The present of LS induces more CH carbonation because of its role as nucleation sites for calcite precipitation, which results in a decrease in SSA, less modification in micro pore volume, but higher CO_2 uptake. Carbonation of samples without limestone filler might results in an increase in specific surface area as a consequence of the opening up of C-S-H porosity. Adding limestone filler also reduces the leaching rate as results of finer initial microstructure.

Acknowledgements

The financial support by Belgian Nuclear Research Centre (SCK•CEN) is gratefully acknowledged.

References

[1] Atis CD. Accelerated carbonation and testing of concrete made with fly ash. Constr Build Mater. 2003;17(3):147-152.
[2] Haga K, Shibata M, Hironaga M, Tanaka S, Nagasaki S. Change in pore structure and composition of hardened cement paste during the process of dissolution. Cement and Concrete Research. 2005;35(5):943-950.
[3] Jain J, Neithalath N. Analysis of calcium leaching behavior of plain and modified cement pastes in pure water. Cement and Concrete Composites. 2009;31(3):176-185.
[4] Dhir RK, Limbachiya MC, McCarthy MJ, Chaipanich A. Evaluation of Portland limestone cements for use in concrete construction. Mater Struct. 2007;40(5):459-473.
[5] Courard L, Michel F. Limestone fillers cement based composites: Effects of blast furnace slags on fresh and hardened properties. Constr Build Mater. 2014;51(0):439-445.
[6] Tsivilis S, Chaniotakis E, Kakali G, Batis G. An analysis of the properties of Portland limestone cements and concrete. Cement Concrete Comp. 2002;24(3-4):371-378.
[7] Lollini F, Redaelli E, Bertolini L. Effects of portland cement replacement with limestone on the properties of hardened concrete. Cement and Concrete Composites. 2014;46(0):32-40.
[8] Phung QT. Effect of Chemical Degradation on Microstructural Changes and Transport Properties of Concrete - Phenomenological Study. 14th FEA PhD Symposium. Ghent University, Belgium2013.
[9] Phung QT. Effects of Carbonation and Calcium Leaching on Microstructure and Transport Properties of Cement Pastes [PhD thesis]. Belgium: Ghent University; 2015.
[10] Phung QT, Maes N, De Schutter G, Jacques D, Ye G. Determination of water permeability of cementitious materials using a controlled constant flow method. Constr Build Mater. 2013;47(0):1488-1496.
[11] Phung QT, Maes N, Jacques D, Bruneel E, Van Driessche I, Ye G, et al. Effect of limestone fillers on microstructure and permeability due to carbonation of cement pastes under controlled CO2 pressure conditions. Constr Build Mater. 2015;82(0):376-390.
[12] Phung QT, Maes N, Jacques D, De Schutter G, Ye G. Investigation of the changes in microstructure and transport properties of leached cement pastes accounting for mix composition. Cement and Concrete Research. 2015.
[13] Kinoshita H, Circhirillo C, SanMartin I, Utton CA, Borges PHR, Lynsdale CJ, et al. Carbonation of composite cements with high mineral admixture content used for radioactive waste encapsulation. Miner Eng. 2014;59(0):107-114.
[14] Han YS, Hadiko G, Fuji M, Takahashi M. Factors affecting the phase and morphology of $CaCO_3$ prepared by a bubbling method. J Eur Ceram Soc. 2006;26(4–5):843-847.
[15] Fernández-Carrasco L, Torréns-Martín D, Martínez-Ramírez S. Carbonation of ternary building cementing materials. Cement and Concrete Composites. 2012;34(10):1180-1186.